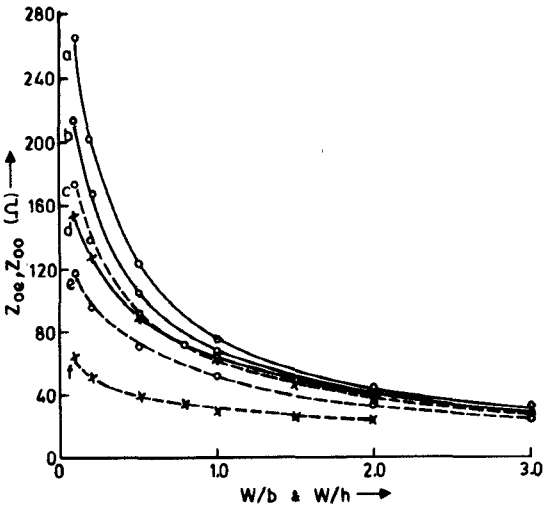

Fig. 5. Variation of even- and odd-mode impedances as a function of W/b and W/h for coupled warped striplines and microstrip lines, respectively.
∘ ∘ ∘ Cohn
× × × Bryand and Weiss
——— even-mode characteristic impedance
---- odd-mode characterisitc impedance

Curve	Description	ϵ_1	ϵ_2	S/b	S/h
a, e	Coupled warped striplines	1.0	1.0	0.1	—
b, c	Coupled warped striplines	1.0	1.0	0.5	—
d, f	Coupled warped microstriplines	10.0	1.0	—	0.2

where S is the edge to edge separation of the planar strips. When $\eta_1 = 0$

$$\eta_3 - \eta_1 + \frac{\eta_4 - \eta_3}{2} = \left(\frac{\pi}{2} - \frac{S}{2a_1} - \frac{W}{2a_1}\right).$$

It can be further approximated that

$$\xi_o - \xi_1 = \ln\left[1 + \frac{p_1}{a_1}\right] = \frac{p_1}{a_1} = A_1 \tag{15a}$$

$$\xi_2 - \xi_o = \ln\left[\frac{1 + p_2/a_1}{1 + p_1/a_1}\right] = \frac{p_2 - p_1}{a_1} = A_2. \tag{15b}$$

In this case, the expressions for the even- and odd-mode impedances of warped coupled striplines reduce to the from

$$Z_{oe} = 480 \cdot \left\{ \sum_{n=0}^{\infty} \frac{J_o^2(m_e\beta_1)\,\mathrm{Sin}^2\left[m_e\left(\frac{\pi}{2} - \beta_1 - \frac{S}{2a_1}\right)\right]}{(2n+1)[\epsilon_1\,\mathrm{Coth}(m_eA_1) + \epsilon_2\,\mathrm{Coth}(m_eA_2)]} \right.$$

$$\left. \cdot \sum_{n=0}^{\infty} \frac{J_o^2(m_e\beta_1)\,\mathrm{Sin}^2\left[m_e\left(\frac{\pi}{2} - \beta_1 - \frac{S}{2a_1}\right)\right]}{(2n+1)[\mathrm{Coth}(m_eA_1) + \mathrm{Coth}(m_eA_2)]} \right\}^{1/2} \tag{16}$$

$$Z_{oo} = 240 \cdot \left\{ \sum_{n=0}^{\infty} \frac{J_o^2(m_o\beta_1)\,\mathrm{Sin}^2\left[m_o\left(\frac{\pi}{2} - \beta_1 - \frac{S}{2a_1}\right)\right]}{n[\epsilon_1\,\mathrm{Coth}(m_oA_1) + \epsilon_2\,\mathrm{Coth}(m_oA_2)]} \right.$$

$$\left. \cdot \sum_{n=0}^{\infty} \frac{J_o^2(m_o\beta_1)\,\mathrm{Sin}^2\left[m_o\left(\frac{\pi}{2} - \beta_1 - \frac{S}{2a_1}\right)\right]}{n[\mathrm{Coth}(m_oA_1) + \mathrm{Coth}(m_oA_2)]} \right\}^{1/2}. \tag{17}$$

Using (16) and (17), the variation of even- and odd-mode impedances with W/b is computed for a symmetric stripline with $\epsilon_1 = \epsilon_2 = 1.0$, $p_1/a_1 = 0.005$, $p_2/a_1 = 0.01$, $\eta_1 = 0.0$, and $S/b = 0.1, 0.5$ as a parameter and the results are presented in Fig. 5. For the sake of comparison, the numerical results obtained by Cohn for a planar structure [7] are also presented in the same figure in the form of circles.

Following similar procedure, the variation of even- and odd-mode impedances of a microstripline is computed as a function of W/h ($h = p_1$) for $\epsilon_1 = 10.0$, $\eta_1 = 0.0$, $p_1/a_1 = 0.01$, and $S/h = 0.2$ and the results are presented in Fig. 5. The results obtained by Bryant and Weiss [8] for a planar structure are also presented in the same figure in the form of crosses. There is a good agreement betweens the two sets of results.

IV. Conclusion

Agreement between the results obtained by the present method for the warped coupled strip- and microstriplines with those of Cohn for a planar symmetric coupled stripline, as well as Bryant and Weiss for a planar coupled microstripline, justifies the validity of the analysis. It is worthwhile to mention that computation is also made for $\eta_1 = 10^0$ and the deviation of corresponding numerical results from those for $\eta_1 = 0^0$ is negligibly small. The advantage of the method of analysis presented in this paper is that the same general formulation developed for coupled elliptical stripline structure can be applied to the coupled cylindrical strip- and microstriplines of elliptic and circular cross section. The method of analysis presented in the paper has enabled evaluation of even- and odd-mode impedance for different dielectrics on the two sides of the coupled strips.

References

[1] Y. C. Wang, "Cylindrical and cylindrically warped strip and microstriplines," *IEEE Trans. Microwave Theory Tech.*, vol. MTT-26, pp. 20–23, Jan. 1978.
[2] K. K. Joshi and B. N. Das, "Analysis of elliptic and cylindrical striplines using Laplace's equation," *IEEE Trans. Microwave Theory Tech.*, vol. MTT-28, pp. 381–386, Apr. 1980.
[3] K. K. Joshi, J. S. Rao, and B. N. Das, "Characteristic impedance of nonplanar striplines," *Inst. Elec. Eng. Proc.* Pt.H, *Microwaves, Optics and Antennas*, vol. 127, no. 5, pp. 287–291, Aug. 1980.
[4] B. N. Das, A. Chakraborty, and K. K. Joshi, "Characteristic impedance of elliptic cylindrical strip and microstriplines filled with layered substrate," *Inst. Elec. Eng., Pt.H, Microwaves, Optics and Antennas*, vol. 130, no. 4, June 1983.
[5] R. E. Collin, *Field Theory of Guided Waves*. New York: McGraw-Hill, 1960.
[6] E. Yamashita and K. Atsuki, "Stripline with rectangular outer conductor and three dielectric layers," *IEEE Trans. Microwave Theory Tech.*, vol. MTT-18, pp. 238–244, May 1970.
[7] S. B. Cohn, "Shielded coupled-strip transmission line," *IRE Trans. Microwave Theory Tech.*, vol. MTT-3, pp. 29–38, Oct. 1955.
[8] T. G. Bryant and J. A. Weiss, "Parameters of microstrip transmission lines and of coupled pairs of microstrip lines," *IEEE Trans. Microwave Theory Tech.*, vol. MTT-16, p. 1027, Dec. 1968.

Computer-Optimized Multisection Transformers between Rectangular Waveguides of Adjacent Frequency Bands

FRITZ ARNDT, SENIOR MEMBER, IEEE, ULRICH TUCHOLKE, AND THOMAS WRIEDT

***Abstract*—Design data are given for multisection double-plane step transformers between *X*- (8.2–12.4 GHz), *Ku*- (12.4.–18 GHz), *K*-**

Manuscript received January 3, 1984; revised June 19, 1984.
The authors are with the Microwave Department, University of Bremen, Kufsteiner Strasse, NW 1, D-2800 Bremen 33, West Germany.

0018-9480/84/1100-1479$01.00 ©1984 IEEE

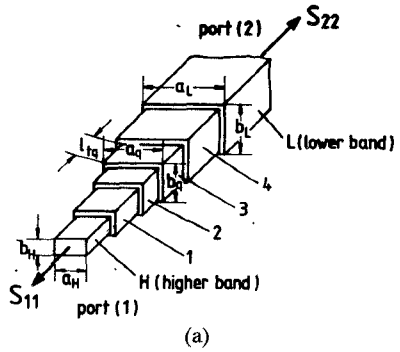

(a)

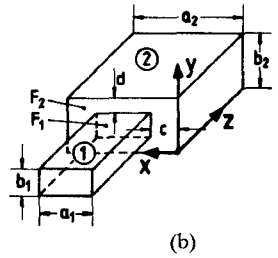

(b)

Fig. 1. Double-plane step transformer. (a) Four-section transformer between a higher and a lower band waveguide. S_{11} = input reflection coefficient at the higher band side, S_{22} = input reflection coefficient at the lower band side. (b) Single-step discontinuity.

(18–26.5 GHz), and *Ka*- (26.5–40 GHz) band waveguides. The calculations, based on a field expansion into orthogonal eigenmodes, take into account the influence of higher order modes. For frequency ranges other than the bands given, simple scaling formulas based on the optimized data yield transformer designs with sufficiently low VSWR. Optimum short transformers are possible if the total transformer length is included within the error function to be optimized. Measurements agree with theory.

I. Introduction

Double-plane step transformers (Fig. 1(a)) are common microwave circuits [1] used to match rectangular waveguides having different heights and widths. Direct design of correct transformer section lengths is not possible using transmission-line theory [1]–[3]. Consequently, individual measurements at each junction are usually required [1]. For computer-aided designs which lead directly to suitable prototypes, therefore, exact field theory methods [4] are necessary. The recent interest in modal analysis solutions of the concentric double-step problem [5], [6] (although previously solved—even for the general excentric case [4], [7]) seems to confirm this need.

Based on the theory given in [4], this paper introduces computer-optimized design tables for multisection transformers between *X*-, *Ku*-, *K*-, and *Ka*-band waveguides.[1] Calculations show that, already for the four-section case,the input reflection coefficient is less than about five percent (i.e., a VSWR of about 1.1) within an approximate frequency band of 1.3:1. The frequency range of unambiguous waveguide application is determined by mode cutoff frequencies of the adjacent waveguide bands (TE_{10} cutoff of the higher band and TE_{20} cutoff of the lower band). Because of the inhomogeneous character of the double-plane step discontinuities, simple scaling formulas for transforming design data to other frequency ranges do not yield optimum results. Nevertheless, the deviations may be tolerable for many practical applications, as is demonstrated by two examples.

[1] *X*-band: 8.2–12.4 GHz; *Ku*-band: 12.4–18 GHz; *K*-band: 18–26.5 GHz; and *Ka*-band: 26.5–40 GHz.

If the total length is not restricted, the computer optimization yields transformer sections which are within a deviation of about forty percent of one quarter wavelength at the midband frequency. For other applications (e.g., satellite communication), however, shorter designs may be advantageous. Therefore, by including the total length in the optimization process, an optimum short two-section transformer between *K*- and *Ku*-band waveguides is found and fabricated as a design example. Measurements agree well with theory if mechanical tolerances are included in the computation.

II. Theory

The theory is given in abbreviated form only; for details, the reader is referred to [4].

For the double-plane step (Fig. 1(b)), the fields

$$\vec{E} = -j\omega\mu\nabla\vec{\Pi}_{hz} + \nabla\times\nabla\vec{\Pi}_{ez}$$
$$\vec{H} = j\omega\epsilon\nabla\times\vec{\Pi}_{ez} + \nabla\times\nabla\vec{\Pi}_{hz} \tag{1}$$

are derived from the axial components of the magnetic and electric Hertzian vector potentials $\vec{\Pi}_h$ and $\vec{\Pi}_e$, respectively. These potentials are assumed to be a sum of suitable eigenmodes satisfying the vector Helmholtz equation and the boundary conditions in waveguide sections 1 and 2 (denoted by the superscript ν):

$$\Pi_{hz}^{(\nu)} = \sum_{m=0}^{M}\sum_{n=0}^{N} A_{hmn}^{(\nu)} T_{hmn}^{(\nu)} \cdot\exp\left(-\gamma_{hmn}^{(\nu)} z\right) + B_{hmn}^{(\nu)} T_{hmn}^{(\nu)} \exp\left(+\gamma_{hmn}^{(\nu)} z\right)$$
$$\Pi_{ez}^{(\nu)} = \sum_{m=1}^{M}\sum_{n=1}^{N} A_{emn}^{(\nu)} T_{emn}^{(\nu)} \cdot\exp\left(-\gamma_{emn}^{(\nu)} z\right) + B_{emn}^{(\nu)} T_{emn}^{(\nu)} \exp\left(+\gamma_{emn}^{(\nu)} z\right) \tag{2}$$

where M and N are the number of modes considered.

The eigenfunctions $T^{(\nu)}$ are normalized [8] so that the power carried by a given wave is proportional to the square of the absolute value of the amplitude coefficients A, B

$$T_{hpl}^{(1)} = \frac{2\cdot\cos\left(k_{xp}^{(1)}\cdot(x-c)\right)\cdot\cos\left(k_{yl}^{(1)}\cdot(y-d)\right)}{D_1\cdot\sqrt{1+\delta_{o,p}}\cdot\sqrt{1+\delta_{o,l}}}$$
$$T_{epl}^{(1)} = \frac{2\cdot\sin\left(k_{xp}^{(1)}\cdot(x-c)\right)\cdot\sin\left(k_{yl}^{(1)}\cdot(y-d)\right)}{D_1}$$
$$T_{hij}^{(2)} = \frac{2\cdot\cos\left(k_{xi}^{(2)}\cdot x\right)\cdot\cos\left(k_{yj}^{(2)}\cdot y\right)}{D_2\cdot\sqrt{1+\delta_{o,i}}\cdot\sqrt{1+\delta_{o,j}}}$$
$$T_{eij}^{(2)} = \frac{2\cdot\sin\left(k_{xi}^{(2)}\cdot x\right)\cdot\sin\left(k_{yj}^{(2)}\cdot y\right)}{D_2} \tag{3}$$

where $m=p$ and $n=l$ for $\nu=1$; $m=i$ and $n=j$ for $\nu=2$ with

$$D_1 = \sqrt{a_1\cdot b_1}\cdot\sqrt{k_x^{(1)^2}+k_y^{(1)^2}}$$
$$D_2 = \sqrt{a_2\cdot b_2}\cdot\sqrt{k_x^{(2)^2}+k_y^{(2)^2}}$$
$$k_{xm}^{(1)} = \frac{p\cdot\pi}{a_1} \quad k_{yn}^{(1)} = \frac{l\cdot\pi}{b_1}, \qquad m=p,\ n=l$$
$$k_{xm}^{(2)} = \frac{i\cdot\pi}{a_2} \quad k_{yn}^{(2)} = \frac{j\cdot\pi}{b_2}, \qquad m=i,\ n=j \tag{4}$$

where $a_1 \leqslant a_2$, $b_1 \leqslant b_2$ (cf., Fig. 1(b)) and

$$\gamma_{h,emn}^{(\nu)} = jk\sqrt{1-\frac{\left(k_{xm}^{(\nu)}\right)^2+\left(k_{yn}^{(\nu)}\right)^2}{k^2}}$$

$k = \omega\sqrt{\mu\epsilon}$ and $\delta_{o,r}$ = Kronecker delta

($r = p, l, i$, and j, respectively). (5)

The still-unknown coefficients A and B in (2) correspond directly to normalized incident and reflected waves, respectively, and are related to each other by the scattering matrix

$$\begin{pmatrix} B^{(1)} \\ B^{(2)} \end{pmatrix} = (S)\begin{pmatrix} A^{(1)} \\ A^{(2)} \end{pmatrix} \tag{6}$$

which can be determined by matching the fields at the step discontinuity at $z = 0$ with the areas F_1 and F_2 (cf., Fig. 1(b))

$$E_{x,y|_{F_1}}^{(1)|^{z=0}} = E_{x,y|_{F_1}}^{(2)|^{z=0}} \quad E_{x,y|_{F_2-F_1}}^{(2)|^{z=0}} = 0$$

$$H_{x,y|_{F_1}}^{(1)|^{z=0}} = H_{x,y|_{F_1}}^{(2)|^{z=0}}. \tag{7}$$

The related coupling integrals are given in [4] and are reproduced using the present notation in the Appendix.

For double-plane steps with eccentric axes [4], the incident TE_{10} wave excites all TE_{mn} and TM_{mn} waves. For concentric axes (the usual configuration for transformers (Fig. 1)), the excitation is limited to waves with odd m and even n.

In order to preserve numerical accuracy, the direct combination of the involved scattering matrices at all step discontinuities of the total transformer is used [4], as opposed to the common treatment by transmission matrices. Although analytically somewhat more extensive, this technique leads to matrix elements only containing exponential functions with negative argument [4]; so, the fringing fields due to modes of higher order than the fundamental mode evanesce relatively quickly with distance between adjacent discontinuities. This direct combination of scattering matrices avoids numerical instabilities caused by the otherwise known situation of interacting discontinuities, like interference or resonance effects. Therefore, no further improvement of the analysis is necessary, e.g., by termination of modes by their characteristic admittances [9], [10].

Due to this matrix technique, it has turned out that modes up to the order $M = 5$ and $N = 4$ (cf., (2)), i.e., up to TM_{54} and TE_{54}, are all that are required in the calculations for the designs given in this paper to yield sufficient asymptotic behavior of the scattering coefficients $|S_{ii}|$. This may be verified by Fig. 2 showing the convergence behavior for $|S_{11}| = |S_{22}|$ of a three-section transformer from *Ka*- to *K*-band, as a typical design example, at two different frequencies (Fig. 2(a) and (b)). In spite of the interaction of the discontinuities, the results for $|S_{11}|$ calculated with $M = 5$, $N = 4$ in (2) differ only slightly from the asymptotic value calculated with $M = 13$, $N = 12$. Similar results may be stated by other examples. Fig. 2(a) indicates further that the order M of the modes has a more severe influence on the convergence behavior than N. This is due to the fact that, between the discontinuities, modes have to be taken into account in succession of increasing cutoff frequencies: TE_{10}, TE_{30}, TE_{12}, TM_{12}, TE_{32}, TM_{32}, TE_{50}, etc. Finally, as may be stated in comparison of Fig. 2(a) with Fig. 2(b), the order of modes necessary does not vary considerably with frequency, since the matrix technique chosen eliminates resonance effects which occur using the common treatment with transmission matrices.

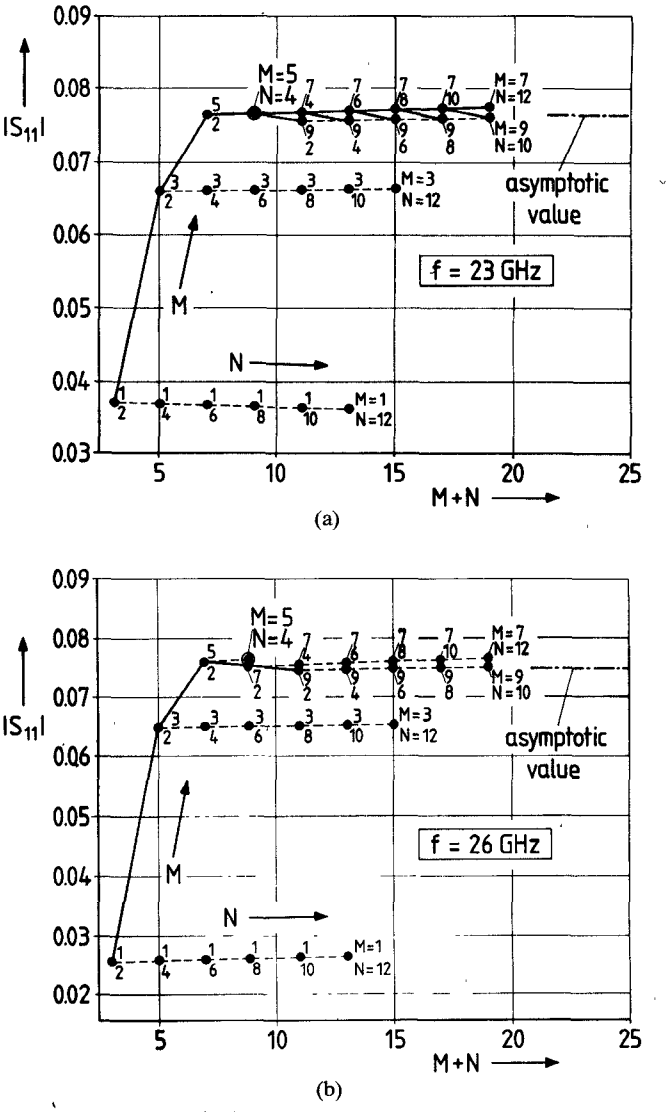

Fig. 2. Convergence behavior of the scattering coefficient $|S_{11}| = |S_{22}|$ of a three-section transformer from *Ka*- to *K*-band (cf., Table I) as a function of the highest mode order M and N, considered in (2). (a) $f = 23$ GHz (the upper number at the calculated points denominates M, the lower denominates N). (b) $f = 26$ GHz. ($M = 5$, $N = 4$ are chosen for the calculations within this paper).

III. Results

Optimized design data for multisection transformers are given in Table I. The values were calculated with the evolution strategy method [11]. The advantages of this method are such that local minima may be found and no differentiation step in the calculation algorithm (like the Fletcher–Powell method) is necessary. The error function

$$F(\bar{x}) = \sum_{u=1}^{U} \frac{|S_{11}(\bar{x}, f_u)|^2}{|S_{21}(\bar{x}, f_u)|^2} \tag{8}$$

is minimized with respect to the parameter vector

$$\bar{x} = \left(a_1, a_2, \cdots, a_Q; b_1, b_2, \cdots, b_Q; l_{t1}, l_{t2}, \cdots, l_{tQ}\right)^T.$$

f_u are frequency sample points, a_q, b_q, and l_{tq} are, respectively, the width, the height, and the length of the qth transformer section, and S_{11}, S_{21} are scattering parameters. The number of frequency sample points U was chosen to be equal to 7. The time for the optimization of one set of transformer parameters is about 60 min for a four-section prototype (Siemens 7880 computer).

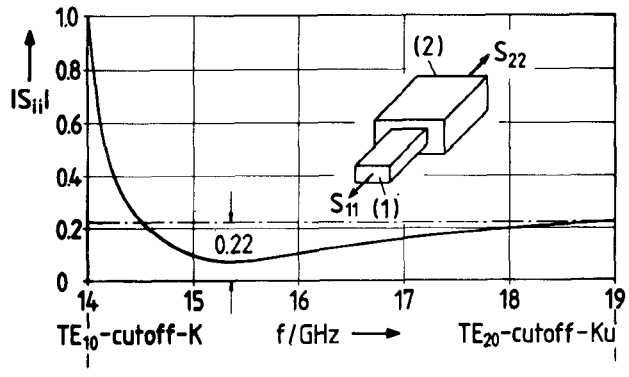

(a)

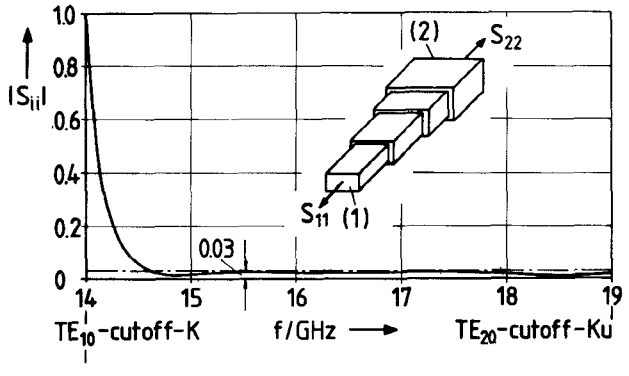

(b)

Fig. 3. Input reflection coefficient $|S_{ii}|$ as function of frequency if a TE_{10}-wave is incident at port $i=1$ or $i=2$, respectively. (a) Single-step discontinuity from *K*- to *Ku*-band (10.7×4.32 mm^2 to 15.8×7.9 mm^2). (b) Two-section transformer (cf., Table I) between *K*- to *Ku*-band.

TABLE I

COMPUTER-OPTIMIZED DESIGN DATA FOR ONE- TO FOUR-SECTION TRANSFORMERS BETWEEN RECTANGULAR WAVEGUIDES FOR *Ku* TO *X*, *K* TO *Ku*, *Ka* TO *K* BAND, AND VICE VERSA

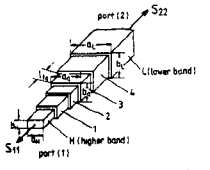

Frequency bands waveguide housings	Number of transformer sections	Transformer dimensions in mm a_q, b_q, l_{tq}													Bandwidth $f_2 - f_1$	Max input reflection $\|S_{11}\|$
		a_1	b_1	l_{t1}	a_2	b_2	l_{t2}	a_3	b_3	l_{t3}	a_4	b_4	l_{t4}			
Ku to X [1] and X to Ku	1	17 66	9 25	11 58											1 32	0 06
	2	16 42	8,56	9,94	18,64	9,58	9,06								1 29	0 03
a_H = 15 8 mm b_H = 7 9 mm a_L = 22 86mm b_L = 10 16mm	3	16,24	8,53	9,12	17 38	9,39	9,56	20 81	10 15	9 15					1 32	0 02
	4	16 44	8 68	9 46	17 73	9 33	9 84	20 67	9 65	8 99	21 72	9 67	7 94		1 32	0 02
K to Ku [1] and Ku to K	1	11 64	5 74	7 19											1 31	0 07
	2	10 85	4 88	7 15	12 19	6 53	7 23								1 31	0 03
a_H = 10 67mm b_H = 4 32mm a_L = 15 8 mm b_L = 7 9 mm	3	10 99	5,05	6,54	12 24	6 52	6 81	14 54	7 49	6 97					1 31	0 03
	4	11 07	5,13	6,99	12,44	6,46	6 34	14 06	6 80	6 39	14 24	6 97	5,34		1 31	0 03
Ka to K [1] and K to Ka	1	7,77	4,06	6 54											1 31	0 1
	2	7 28	3,80	4,72	7 92	4 13	5 02								1 31	0 08
a_H = 7,11mm b_H = 3,56mm a_L = 10,67mm b_L = 4 32mm	3	7 31	3 57	4 30	7 39	3 59	4 62	9 16	4 23	5 01					1 30	0 077
	4	7 37	3 90	4 62	7 79	4 08	4 08	9 41	4 12	4 16	10 65	4 13	3 50		1 30	0 05
K to Ku [1] and Ku to K	2	11 37	5 51	6 56	12 58	6 68	2 70	optimum short, theory							1 32	0 1
a_H = 10,67mm b_H = 4,32mm a_L = 15,8 mm b_L = 7,9 mm	2	11,48	5 59	6 55	12 62	6 90	2 69	optimum short, realized [2] a_H=10 65mm, b_H=4 33mm, a_L=15 91mm, b_L=7 92mm							1 30	0 09

[1] X-band 8.2-12.4 GHz; Ku-band 12.4-18 GHz; K-band 18-26.5 GHz; Ka-band 26.5-40 GHz

[2] measured with measuring microscope

Fig. 3 shows the input reflection coefficient $|S_{ii}|$ as a function of frequency of the TE_{10} wave at port $i=1$ or $i=2$ if a TE_{10} wave is incident at the corresponding waveguide port for the double-step discontinuity from *K*- to *Ku*-band waveguide (Fig. 3(a)). Even a two-section transformer (Table I) between the waveguides reduces the maximum passband value $|S_{ii}|=0.22$ (Fig. 3(a)) to about 0.03 (Fig. 3(b)) within nearly the range of suitable waveguide application, which is limited by the cutoff frequencies of the TE_{20} wave in the broader (*Ku*-band) waveguide and of the TE_{10} wave of the smaller (*K*-band) waveguide. Within this unambiguous range, the TE_{10}-wave reflection coefficient $|S_{22}|$ for a TE_{10}-wave incident at port 2 at the broader waveguide is equal to $|S_{11}|$, the input reflection coefficient at the smaller waveguide at port 1. Since this holds for all design examples in this paper, Table I also may be used for optimum transformers from the broader to the smaller waveguides. Fig. 4 shows the input reflection coefficients of the TE_{10} wave for four-section transformers between *Ka*- and *K*-band (Fig. 4(a)) and *Ku*- and *X*-band (Fig. 4(b)) as examples.

Transformer designs for waveguide dimensions other than the standard *Ka*- to *X*-band values considered in Table I can be obtained using the simple scaling relations given as follows:

$$\frac{a_{q\,\mathrm{opt}}-a_H}{a_L-a_H}=\frac{a_{q\,\mathrm{new}}-a_{H\,\mathrm{new}}}{a_{L\,\mathrm{new}}-a_{H\,\mathrm{new}}}$$
$$\frac{b_{q\,\mathrm{opt}}-b_H}{b_L-b_H}=\frac{b_{q\,\mathrm{new}}-b_{H\,\mathrm{new}}}{b_{L\,\mathrm{new}}-b_{H\,\mathrm{new}}} \tag{9}$$

where

$a_{q\,\mathrm{new}}, b_{q\,\mathrm{new}}$ = qth transformer section width and height,
$a_{H\,\mathrm{new}}, b_{H\,\mathrm{new}}, a_{L\,\mathrm{new}}, b_{L\,\mathrm{new}}$ = actual higher (H)- and lower (L)-band waveguide dimensions,
a_H, b_H, a_L, b_L = higher (H)- and lower (L)-band waveguide dimensions in Table I which are in the proximity of $a_{H\,\mathrm{new}}$ etc.,
$a_{q\,\mathrm{opt}}, b_{q\,\mathrm{opt}}$ = related optimum transformer dimensions in Table I.

The transformer section lengths l_{tq} are scaled in relation to the ratio of the old to the new arithmetic midband guide wavelength λ_{go}. This simple frequency transformation, if applied to the a, b dimensions (instead of (9)), would lead to poorer input reflection factor results. Moreover, (9) automatically includes the dimensions of the new lower and higher band waveguides and guarantees nearly the same bandwidth behavior of the transformer.

The transformer dimensions interpolated with (9) yield sufficiently low input reflection values, although not as good as the computer-optimized results. This is demonstrated in Fig. 5(a) and (b) for two three-section transformer examples (from *Ku*- to *X*-band and *Ka*- to *K*-band) based on the optimized *K*- to *Ku*-band design (Table I).

If the total transformer length is included in the error function (8), optimum short transformers are possible. Fig. 6(a) shows an example of a two-section transformer between *K*- and *Ku*-band waveguides, which is about 36 percent shorter than the "quarter-wave"-type of Table I. In this example, the frequency behavior is nearly the same and the absolute input reflection values are only about twice as high (solid versus dashed line). Fig. 6(b) shows a photograph of the actual short section transformer used to obtain the experimental results. The measurements agree

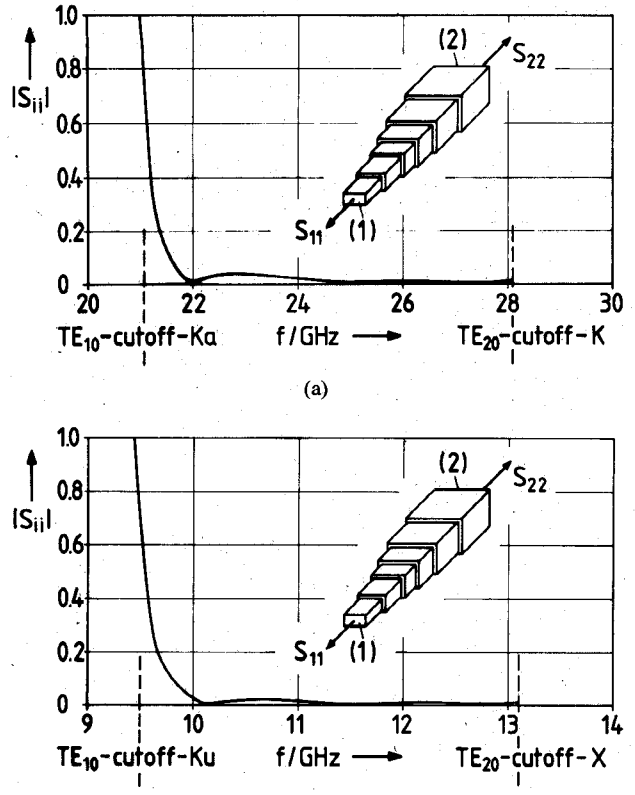

Fig. 4. Input reflection coefficient $|S_{ii}|$ at port 1 as a function of frequency if a TE_{10}-wave is incident at port $i=1$ or $i=2$, respectively. (a) Four-section transformer (cf., Table I) between *Ka*- and *K*-band. (b) Four-section transformer (cf., Table I) between *Ku*- and *X*-band.

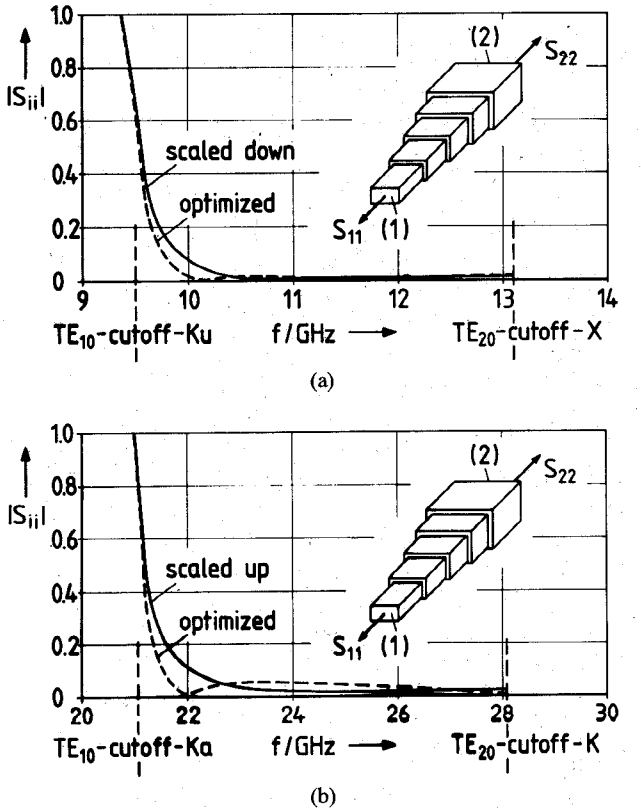

Fig. 5. Input reflection coefficient $|S_{ii}|$ at port i as a function of frequency of a three-section transformer. ---- optimized (Table I) ——— scaled down or up, respectively, according to (9) with optimized *K*- to *Ku*-band results. (a) *Ku*- to *X*-band, and (b) *Ka*- to *K*-band.

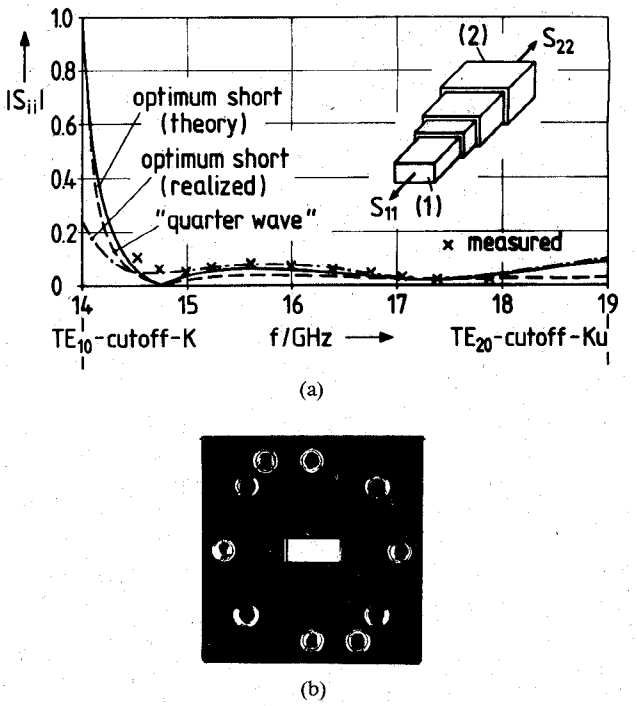

Fig. 6. Optimum short two-section transformer between *K*- and *Ku*-band (Table I). (a) Input reflection coefficient $|S_{ii}|$ at port i as a function of frequency, (b) photograph.

well with theory (Fig. 6(a)) if the actual dimensions (measured with a microscope) are included in the computations. The mechanical tolerances are 0.08 mm.

IV. Conclusion

Computer-aided design of multisection double-plane step transformers between rectangular waveguides of different heights and widths is performed by including the higher order mode excitation effects in the theory. In contrast to *E*-plane or *H*-plane stepped transformers, double-plane step circuits require all six field components to be considered. The orthogonal expansion method used in the calculations shows sufficient asymptotic behavior of the input reflection results if all modes up to TM_{54} and TE_{54} are included. An error function, numerically minimized, yields one- to four-section transformer dimensions between the standard waveguide bands (*X* to *Ku*, *Ku* to *K*, *K* to *Ka*, and vice versa). For other frequency bands, simple scaling formulas based on the optimized data yield transformer designs with sufficiently low reflection coefficients. If the total transformer length is included in the optimization process, optimum short transformer sections are obtained. This is demonstrated by a *Ku*- to *K*-band two-section prototype, which is about 36 percent shorter than its "quarter-wave" counterpart. Measurements agree well with theory if the mechanical tolerances are included.

Appendix

Coupling integrals related to (7) (cf., [4])

$$V_{hhijpl}=\sqrt{\frac{\gamma_{hij}^{(2)}}{\gamma_{hpl}^{(1)}}}\int_{F_1}\left(-\vec{e}_{hpl}^{(1)}\right)\left(-\vec{e}_{hij}^{(2)}\right)dx\,dy \qquad \text{(A1)}$$

$$-V_{heijpl}=\frac{\sqrt{\gamma_{hij}^{(2)}\gamma_{epl}^{(1)}}}{j\dfrac{2\pi}{\lambda}}\int_{F_1}\left(\vec{e}_{epl}^{(1)}\right)\left(-\vec{e}_{hij}^{(2)}\right)dx\,dy=0 \qquad \text{(A2)}$$

$$-V_{ehijpl}=\frac{j\frac{2\pi}{\lambda}}{\sqrt{\gamma_{hpl}^{(1)}\gamma_{eij}^{(2)}}}\int_{F_1}\left(-\vec{e}_{hpl}^{(1)}\right)\left(\vec{e}_{eij}^{(2)}\right)dx\,dy \tag{A3}$$

$$V_{eeijpl}=\sqrt{\frac{\gamma_{epl}^{(1)}}{\gamma_{eij}^{(2)}}}\int_{F_1}\left(\vec{e}_{epl}^{(1)}\right)\left(\vec{e}_{eij}^{(2)}\right)dx\,dy \tag{A4}$$

where F_1 = area of waveguide 1 (see Fig. 1(b)). The vectors $\vec{e}$ denote

$$\vec{e}_{hpl}^{(1)}=\vec{e}_z\times\nabla_{xy}T_{hpl}^{(1)} \tag{A5}$$

$$\vec{e}_{epl}^{(1)}=\nabla_{xy}T_{epl}^{(1)} \tag{A6}$$

$$\vec{e}_{hij}^{(2)}=\vec{e}_z\times\nabla_{xy}T_{hij}^{(2)} \tag{A7}$$

$$\vec{e}_{eij}^{(2)}=\nabla_{xy}T_{eij}^{(2)}. \tag{A8}$$

References

[1] G. Matthaei, L. Young, and E. M. T. Jones, *Microwave Filters, Impedance-Matching Networks, and Coupling Structures*. New York: McGraw-Hill, 1964.

[2] S. B. Cohn, "Optimum design of stepped transmission-line transformers," *IRE Trans. Microwave Theory Tech.*, vol. MTT-3, pp. 16–21, Apr 1955.

[3] H. J. Riblet, "General synthesis of quarter-wave impedance transformers," *IRE Trans. Microwave Theory Tech.*, vol. MTT-5, pp. 36–43, 1957.

[4] H. Patzelt, and F. Arndt, "Double-plane steps in rectangular waveguides and their application for transformers, irises, and filters," *IEEE Trans. Microwave Theory Tech.*, vol. MTT-30, pp. 771–776, May 1982.

[5] R. Safavi-Naini and R. H. MacPhie, "Scattering at rectangular-to-rectangular waveguide junctions," *IEEE Trans. Microwave Theory Tech.*, vol. MTT-33, pp. 2060–2063, Nov. 1982.

[6] Y. C. Shih and K. G. Gray, "Convergence of numerical solutions of step-type waveguide discontinuity problems by modal analysis," in *1983 MTT-S Int. Microwave Symp. Dig.* (Boston), pp. 233–235.

[7] H. Patzelt and F. Arndt, "Mehrstufige inhomogene Rechteck-Hohlleitertransformatoren," *Frequenz*, vol. 32, pp. 233–239, Aug. 1978.

[8] R. E. Collin, *Field Theory of Guided Waves*. New York: McGraw-Hill, 1960.

[9] M. S. Navarro, T. E. Rozzi, and Y. T. Lo, "Propagation in a rectangular waveguide periodically loaded with resonant irises," *IEEE Trans. Microwave Theory Tech.*, vol. MTT-28, pp. 857–865, Aug. 1980.

[10] T. Rozzi, "A new approach to the network modeling of capacitive irises and steps in waveguide," *Int. J. Circuit Theory Appl.*, vol. 3, pp. 339–354, Dec. 1975.

[11] H. Schmiedel, "Anwendung der Evolutionsoptimlerung bei Milrowellenschaltungen," *Frequenz*, vol. 35, pp. 306–310, Nov. 1980.

Analysis of Finline with Finite Metallization Thickness

TOSHIHIDE KITAZAWA AND RAJ MITTRA, FELLOW, IEEE

***Abstract*—In this paper, we present a method for analyzing finline structures with finite metallization thickness. The method is based on a hybrid mode formulation but it by-passes the lengthy process of formulating the determinantal equation for the unknown propagation constant. Some numerical results are presented to show the effect of the metallization thickness for unilateral and bilateral finlines.**

Manuscript received October 6, 1983; revised June 11, 1984. This work was supported in part by DAAG29-82-K-0084 and JSEP N000-1479C-0424.

The authors are with the Electrical Engineering Department, University of Illinois, Urbana, IL. T. Kitazawa is on leave from the Kitami Institute of Technology, Kitami, Japan.

I. Introduction

Finline structures have received considerable attention because of their usefulness as millimeter-wave integrated-circuit components. Recently, two efficient numerical methods for analyzing the propagation characteristics of finline structures were presented. The first of these employs the spectral-domain technique [1], [2], whereas the second utilizes network analytical methods for electromagnetic fields [3]. Both of these methods are based on the hybrid mode formulation, but they neglect the effect of the metallization thickness, which increases with higher operating frequencies and narrower gaps in the metallization. An eigenvalue equation for a unilateral finline with a finite metallization thickness has been previously derived [4] using the hybrid mode formulation, but only approximate results based on the TE-approximation have been presented in the above paper. In this paper, we discuss an efficient hybrid mode formulation for the finite metallization problem and derive the solution to the problem without resorting to the TE-approximation. Although the method is an extension of the treatment in [3], [5], and [6], it derives Green's functions using the conventional circuit theory rather than by directly solving the differential equations with boundary conditions.

II. The Network Formulation of the Problem

The unilateral finline shown in Fig. 1 is used to illustrate the formulation procedure, but the method itself is quite general.

As a first step, we express the transverse (to z) fields in each region by the following spectral representation:

$$\left.\begin{matrix}\bar{E}_t^{(i)}(x,y,z)\\ \bar{H}_t^{(i)}(x,y,z)\end{matrix}\right\}=\sum_{l=1}^{2}\sum_{n=0}^{\infty}\left\{\begin{matrix}V_{ln}^{(i)}(z)\bar{f}_{ln}^{(i)}(x)\\ I_{ln}^{(i)}(z)\bar{g}_{ln}^{(i)}(x)\end{matrix}\right\}e^{-j\beta_0 y},\qquad i=1,2,3,4 \tag{1}$$

where the vector mode functions $\bar{f}_{ln}^{(i)}$ and $\bar{g}_{ln}^{(i)}$ in each region are given as

A) region (1), (3), and (4)

$$\bar{f}_{1n}^{(i)}=\frac{-1}{K_A}\sqrt{\frac{\eta_n}{2A}}\left\{\bar{x}_0\alpha_A\cos(\alpha_A x)-\bar{y}_0 j\beta_0\sin(\alpha_A x)\right\}$$

$$\bar{f}_{2n}^{(i)}=\frac{1}{K_A}\sqrt{\frac{\eta_n}{2A}}\left\{\bar{x}_0 j\beta_0\cos(\alpha_A x)-\bar{y}_0\alpha_A\sin(\alpha_A x)\right\}$$

$$\bar{g}_{ln}^{(i)}=\bar{z}_0\times\bar{f}_{ln}^{(i)}\qquad(l=1,2)$$

$$\alpha_A=\frac{n\pi}{A},\quad K_A=\sqrt{\alpha_A^2+\beta_0^2}$$

$$\eta_n=\begin{cases}1\ (n=0)\\ 2\ (n\neq 0)\end{cases}. \tag{2}$$

B) region (2)

$$\bar{f}_{1n}^{(2)}=\frac{-1}{K_W}\sqrt{\frac{\eta_n}{2W}}\left\{\bar{x}_0\alpha_W\cos(\alpha_W x)-\bar{y}_0 j\beta_0\sin(\alpha_W x)\right\}$$

$$\bar{f}_{2n}^{(2)}=\frac{1}{K_W}\sqrt{\frac{\eta_n}{2W}}\left\{\bar{x}_0 j\beta_0\cos(\alpha_W x)-\bar{y}_0\alpha_W\sin(\alpha_W x)\right\}$$

$$\bar{g}_{ln}^{(2)}=\bar{z}_0\times\bar{f}_{ln}^{(2)}\qquad(l=1,2),\ \alpha_W=\frac{n\pi}{W},\ K_W=\sqrt{\alpha_W^2+\beta_0^2} \tag{3}$$

where β_0 is the propagation constant, and $\bar{x}_0$, $\bar{y}_0$, and $\bar{z}_0$ are the x-, y-, and z-directed unit vectors, respectively. It should be noted that the vector mode functions $\bar{f}_{\ln}^{(i)}$, $\bar{g}_{\ln}^{(i)}$ satisfy the

0018-9480/84/1100-1484$01.00 ©1984 IEEE